Self-Regeneration Hybrid Hydrogel for Bisphenol A Adsorption in Water

Mingyue Piao
Jilin Normal University
Hongxue Du
Jilin Normal University
Yuwei Sun
Jilin Normal University
Honghui Teng (tenghh888@163.com)
Jilin Normal University https://orcid.org/0000-0002-2191-3752

Research Article

Keywords: Adsorption, Bisphenol A, Hybrid hydrogel, TiO2, Photocatalysis, Regeneration.

Posted Date: September 1st, 2021

DOI: https://doi.org/10.21203/rs.3.rs-661488/v1

Version of Record: A version of this preprint was published at Environmental Science and Pollution Research on January 29th, 2022. See the published version at https://doi.org/10.1007/s11356-022-18833-8.

Self-regeneration hybrid hydrogel for bisphenol A adsorption in water

Mingyue Piao [1,2], Hongxue Du [1], Yuwei Sun [1,2], Honghui Teng [1,2 *]

[1] Key Laboratory of Environmental Materials and Pollution Control, the Education Department of Jilin Province, Jilin Normal University, Siping, China

[2] College of Environmental Science and Engineering, Jilin Normal University, Siping, China

[*] Corresponding author at College of Environmental Science and Engineering, Jilin Normoal University, 1301 Haifeng Road, Siping 136000, China. E-mail address: tenghh888@163.com

.

Abstract

Hybrid hydrogel was synthesized by immobilizing TiO_2 in polyethylene glycol diacrylate (TiO_2@PEGDA) as an efficient adsorbent with photocatalysis property for bisphenol A (BPA) elimination. TiO_2@PEGDA exhibited spherical and rough structure with limited crystallinity and abundant functional groups. The contact angle was 61.96°, indicating that TiO_2@PEGDA is hydrophilic. The swelling capacity of TiO_2@PEGDA (9.0%) was decreased compared with pristine PEGDA (15.6%). Adsorption results demonstrated that the maximum adsorption capacity of TiO_2@PEGDA (101.4 mg/g) for BPA was slightly higher than pristine PEGDA (97.68 mg/g). The adsorption capacity was independent with pH at pH $<$ 8.0, and decreased obviously when the value of pH was higher than 8.0. The adsorption behavior was fitted well with the pseudo-second-order kinetic and the Freundlich isotherm model. Both ΔG_0 and ΔH_0 were negative, indicating that BPA adsorbed on TiO_2@PEGDA was an exothermic and spontaneous process. Regeneration study was performed by photocatalysis, and the adsorption capacity was 85.6% compared with the initial capacity after four cycles of illumination, indicating that TiO_2@PEGDA could be recycled without significant loss of adsorption capacity. Consequently, TiO_2@PEGDA can serve as an eco-friendly and promising material for efficiently adsorbing BPA with self-clean property.

Keywords Adsorption · Bisphenol A · Hybrid hydrogel · TiO_2 · Photocatalysis · Regeneration

Introduction

Bisphenol A (BPA), as one of the most widely used endocrine disruptors, has attracted public attention in recent years since it can disrupt physiological function by mimicking natural hormone effect. Many studies have recognized that BPA may put adverse effect on reproductive function (Wang et al. 2021), obey (Biemann et al. 2021), cancer (Almeida et al. 2021; Sundarraj et al. 2021) and cardiovascular disease (Moon et al. 2021). Furthermore, BPA has been shown to elicit toxicity to plants (Ashfaq et al. 2018). As an important monomer, BPA is widely applied, and inevitably released into natural sources like soils (Xu et al. 2021), sediments (Liu et al. 2021), drinking waters (Santhi et al. 2012) and surface waters (Chakraborty et al. 2021). Consequently, it is necessary to study appropriate methods for BPA removal.

Adsorption is one of the most effective technologies for removing a wide range of pollutants (Mpatani et al. 2021). Hydrogel adsorbents, as a new kind of adsorbent materials, have been widely used to eliminate BPA in water, showing super high adsorption capacity (Chen et al. 2019), fast adsorption equilibrium (Zhou et al. 2019) and wide pH-independence (Du and Piao 2018). BPA adsorbed on β cyclodextrin (β-CD)/hydroxypropyl methylcellulose hydrogel yielded maximum capacity of 14.6 mg/g (de Souza and Petri 2018), and that was 30.77 mg/g for β-CD grafted cellulose bead (Lin et al. 2019). Carbon/MCM-41/alginate hydrogel exhibited superior adsorption capacity for BPA as high as 222.32 mg/g at 50 °C (Marrakchi et al. 2021). Although these hydrogels can achieve ideal adsorption capacity, poor regeneration limits their application because of used adsorbents are classified as hazardous waste materials. In order to overcome the problem of solid wastes generation, solvent extraction is often used to regenerate BPA from used adsorbents. Organic solvents are

the most favorite regeneration liquids due to their high solubility for BPA than acid or alkali solutions (Zhou et al. 2019). However, regeneration liquids still belong to liquid pollutants that have to be treated before disposal.

Photocatalysis is one of the most commonly used advanced oxidation technologies, and it can mineralize a wide range of pollutants. This process use atmospheric oxygen as oxidant, and can be carried out under ambient condition. Thus, immobilizing photocatalytic materials in hydrogel adsorbents is regarded as an extremely effective method to solve regeneration issue (Zhu et al. 2018), avoiding second pollution which derives from used adsorbents or regeneration liquids. Furthermore, it is easy and convenient to immobilize inorganic photocatalytic materials into hydrogels for preparing hybrid adsorbents.

Polyethylene glycol diacrylate (PEGDA), one of the representative photo-cross-linkable monomers, can be cross-linked under UV irradiation in several minutes. We introduced TiO_2 nanoparticles into PEGDA hydrogel by solution mixing in one step for the purpose of fabricating hybrid hydrogels with the property of self-clean regeneration. These added TiO_2 have two roles: (1) as binding agent to adsorb BPA, and (2) as photocatalyst to eliminate BPA under UV exposure for regeneration.

Materials and methods

Chemicals and materials

Light mineral oil, 2-hydroxy-2-methylpropiophenone (HMPP), PEGDA (MW 575) and BPA were purchased from Sigma-Aldrich (USA). Span 80, Tween 20 and TiO_2

were purchased from Aladdin Chemical Co. (China). Deionized water was used throughout this work.

Synthesis of TiO_2@PEGDA

Solution mixing is utilized to prepare hybrid hydrogel, which involves homogeneous dispersion of inorganic material in monomer solution followed by polymerization. The preparation process of TiO_2@PEGDA was displayed in Fig. 1. First, TiO_2 solution was mixed with PEGDA to obtain homogeneous dispersion of TiO_2 throughout PEGDA matrix, and photoinitiator HMPP (1 v%) was mixed together. Then the final mixture acted as water phase was dripped into oil phase for oscillation to form droplets. In order to obtain stable droplets, Span 80 (1 v%) and Tween 20 (1 v%) were added into oil phase. Then these droplets were exposed under UV irradiation of 365 nm (B-100AP, UVP, USA) for 3 min to ensure sufficient cross-linking, and solid hydrogels were obtained. They were centrifuged from oil and washed with detergent to removal oil and unreacted monomers. To evaluate the effect of TiO_2, three different concentrations were used: 1‰, 1% and 10 wt%. The ratio of TiO_2 and PEGDA in water phase was 1:2 (v/v). Light polymerization mechanism consists of three stages: initiation, propagation and termination. Firstly, the initiator HMPP is decomposed into primary radicals under UV exposure, and these radicals swap out H from –OH to form alkoxy radicals. Then alkoxy radicals react with a molecule of monomer (PEGDA) to form the first radical, and the radical reacts with other PEGDA to induce chains growth. Finally, polymer chains will terminate when all the monomers are depleted.

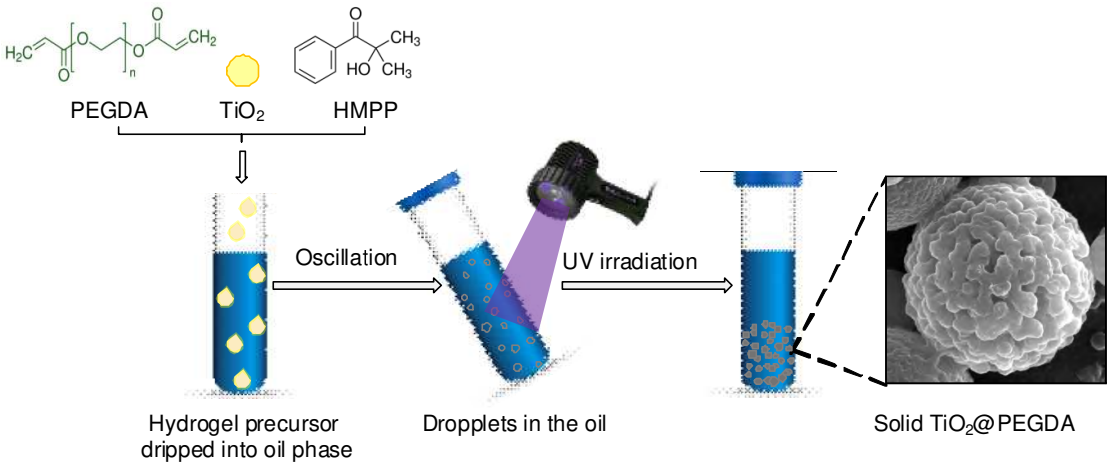

Fig. 1 Diagram for the synthesis of hybrid hydrogels (TiO_2@PEGDA)

Characterization of TiO_2@PEGDA

Hybrid hydrogels were coated with gold to form a thin layer, and imaged by SEM (JSM-7800F, Prime, Japan) under vacuum at 15 kV. FTIR spectrum was scanned from 4000 to 400 cm^{-1} with a resolution of 1 cm^{-1} (Nicolet iS5N, Thermo fisher, USA). Before detection, the powder mixture of ground sample and KBr was compressed into a transparent disk. The crystalline structure was detected by XRD (D/max 2500, Rigaku, Japan) in a range of 2θ = 10–80 ° with Cu Kα radiation (λ = 1.5406 Å, 40 kV, 200 mA). The hydrophilicity was measured by contact angle measuring instrument (OCA200, Dataphysics, Gemany).

Swelling property

Swelling property was determined by gravimetric method. Accurate weighed hydrogels were immersed in 5 mL of water for totally swollen, and then dried the surface water of these water-saturated hydrogels with paper. The swelling ratio was calculated by Eq. (1).

$$Swelling\ \ ratio = \frac{W_{wet} - W_{dry}}{W_{dry}} \times 100\% \quad (1)$$

Where W_{wet} and W_{dry} stand for the mass of wet and dry hydrogels, respectively.

BPA adsorption in water

Adsorption experiments were conducted at 25 °C. Ten milligram of TiO_2@PEGDA was mixed well with 2 mL of BPA (25 mg/L or 500 mg/L) in deionized water by continuous shaking. After equilibrium time, unreacted BPA was separated from the hydrogels by centrifugation, and the equilibrium adsorption capacity (q_e, mg/g) was measured by Eq. (2).

$$q_e = \frac{(C_0 - C_e)}{m} V \quad (2)$$

Where C_0 and C_e (mg/L) stand for the initial and the equilibrium concentration of BPA, respectively. V (mL) and m correspond to the volume of BPA solution and the mass (mg) of the hydrogels, respectively.

BPA was quantified by HPLC which equipped with UV–vis detector (276 nm) and C18 column. The mobile phase was composed of deionized water and acetonitrile (50 v% : 50 v%) with the flow rate of 1.0 mL/min at 30 ℃.

Photocatalysis regeneration of used TiO_2@PEGDA

The regeneration tests were operated by photocatalysis and repeated for 5 times. BPA-saturated TiO_2@PEGDA was light-triggered (500 W Xenon lamp) for 3 h until BPA was totally degraded. Afterwards, the regenerated hydrogels were used for next fresh BPA (500 mg/L) adsorption in deionized water. The regeneration efficiency was calculated by Eq. (3).

$$RE = \frac{q_{e,r}}{q_{e,i}} \times 100\% \quad (3)$$

Where $q_{e,r}$ and $q_{e,i}$ stand for the equilibrium adsorption capacity of regenerated and initial hydrogels, respectively.

All the experiments were repeated three times for errors reduction.

Results and discussions

Characterization of TiO_2@PEGDA

It can be clearly seen in Fig. 2a that the surface of pristine hydrogels was smooth, but it became rough when 10% TiO_2 added (Fig. 2b), offering much higher surfaces for BPA to get inside and combine with the active sites. XRD spectras were presented in Fig. 3, and pristine PEGDA hydrogel exhibited a broad but strong diffraction peak around $2\theta = 21°$, indicating that PEGDA was amorphous with limited crystallinity. TiO_2@PEGDA exhibited anatase phase marked at 25.6°, which was in good according with TiO_2 standard card (JCPDS card No. 65-2448), indicating that TiO_2 were successfully immobilized on PEGDA matrix. FTIR was detected in order to identify functional groups presented on the adsorbent surface. Fig. 4 showed various chemical bonds in pristine PEGDA, including –OH (the absorbance bands at 3318 cm^{-1}), C–H (2871 cm^{-1}), C=O (1734 cm^{-1}) and C–O (1106 cm^{-1}). The intensity of broad absorption band at 3318 cm^{-1} disappeared obviously in TiO_2@PEGDA, indicating that H-bonding interaction was involved in the formation of hybrid hydrogel. The contact angle of pristine PEGDA was 46.73°, and it became 61.96° towards TiO_2@PEGDA, showing that the hydrophilicity of the hydrogel decreased

after TiO_2 were introduced, further indicating that the hydrophilic groups were involved in the formation of TiO_2@PEGDA.

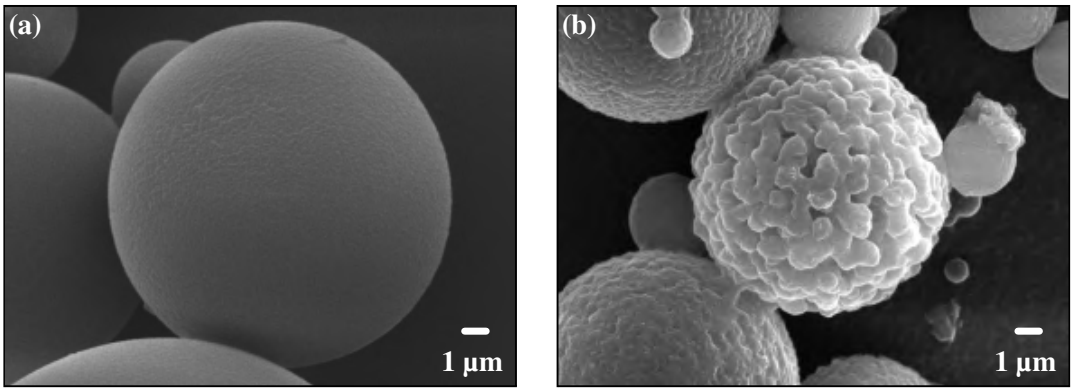

Fig. 2 SEM. **a** Pristine PEGDA. **b** TiO_2@PEGDA

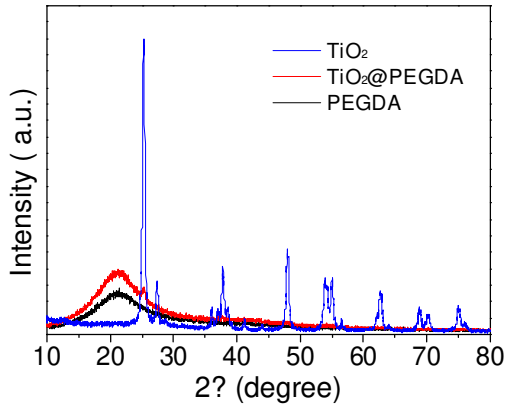

Fig. 3 XRD spectras of TiO_2, pristine PEGDA and TiO_2@PEGDA

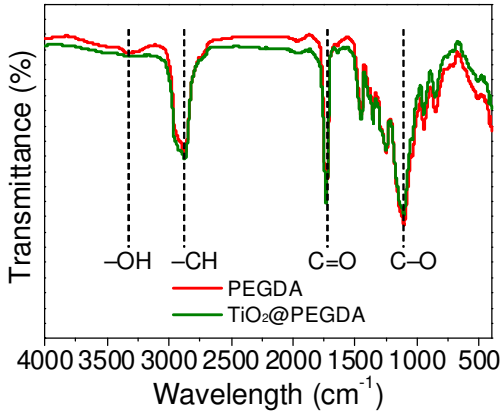

Fig. 4 FTIR spectras of pristine PEGDA and TiO_2@PEGDA

Swelling property

The influence of TiO_2 on the swelling property of the hydrogels was operated in deionized water and the results were shown in Fig. 5. The swelling ratios were

15.60%, 13.40%, 11.96% and 9.00% corresponding to the amount of TiO_2 0, 1‰, 1%, and 10% after equilibrium time, respectively. Pristine hydrogel exhibited the biggest swelling capacity, while hydrogels containing the most TiO_2 had the smallest. By increasing the concentration of TiO_2, there was a reduction in the swelling ratio, may owing to the higher cross-linking density resisted the diffusion of water into the system, because TiO_2 can be acted as cross-linking agent during synthesis process (Glass et al. 2018), and thus cross-linking degree was enhanced. On the other hand, the number of hydrophilic groups in the hydrogel can make a key role in water absorbency ability. Hydroxyls in PEGDA were consumed during preparation of hybrid hydrogels by introducing TiO_2, hence reduced hydroxyls led to decrease the water absorbency, because as hydrophilic group, hydroxyls were easily attract water molecules. In this work, the water uptakes of both pristine PEGDA and TiO_2@PEGDA were much lower than other common hydrogels as summarized in Table 1. PEGDA acted both as monomer and cross-linking agent during preparation, which may leading to the highly polymerization degree of PEGDA-based hydrogels.

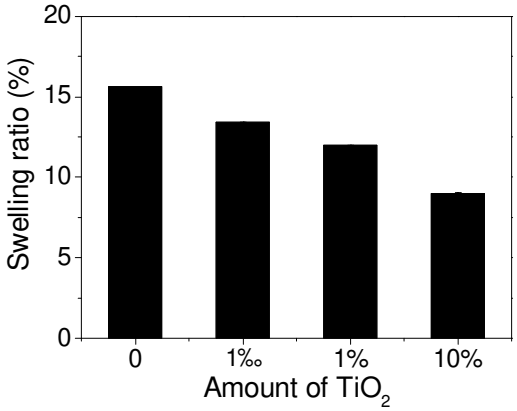

Fig. 5 Swelling ratio of the hydrogels with different amount of TiO_2 loaded

Table 1 Swelling ratio of various hydrogels in deionized water

Hydrogel adsorbents	S_{max} (%)	References
Cellulose/acrylamide/acrylic acid	about 7500	(Dai et al. 2019)
Acrylic acid	11768	(Liu et al. 2019)

Cellulose	1500	(Kumar et al. 2019)
Polyethylene glycol	4670	(Van den Broeck et al. 2019)
PEGDA	15.60	This work
TiO_2@PEGDA	9.00–13.40	This work

196 S_{max}: swelling degree after equilibrium.

197 Adsorption study

198 Effect of TiO_2

199 The influence of TiO_2 on the adsorption capacity was investigated. Hybrid hydrogels
200 adsorption towards BPA maintained the same with pristine hydrogel until the amount
201 of TiO_2 increased to 10%, demonstrating a slightly higher adsorption capacity (101.40
202 mg/g) than pristine PEGDA (97.68 mg/g). Addition of TiO_2 made the surface of
203 hydrogel rough, resulting in an increase of the adsorb active sites. And TiO_2 itself has
204 the ability to adsorb BPA (Hunge et al. 2021). The following adsorption experiments
205 were conducted using TiO_2@PEGDA as adsorbent with 10% TiO_2 added.

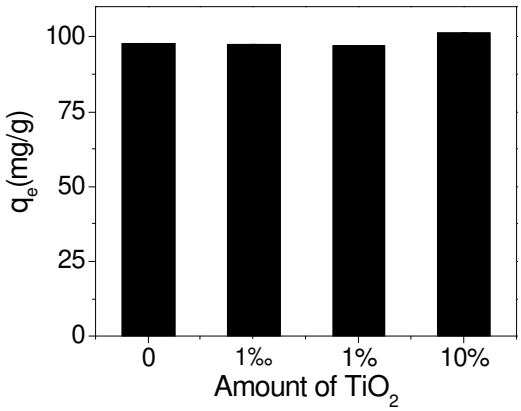

206
207 **Fig. 6** Effect of TiO_2 on BPA adsorption (BPA = 500 mg/L)

208 Effect of pH

209 The solution pH controls the adsorption process of various pollutants, since it not only
210 changes the surface charge of adsorbents, but also affects the

protonation/deprotonation of pollutants according to their pI. Fig. 7 showed that the adsorption ability of TiO_2@PEGDA towards BPA capacity was stable under acidic and neutrality condition, and until pH＞8.0, it decreased obviously from 4.92 mg/g to 3.71 mg/g, indicating that alkaline environment was not conducive to adsorbed BPA by the hydrogels. When pH increased to above 9.0, BPA will be in its deprotonation form because pI of BPA is 9.6–10.2 (Kuo 2009), and thus it is difficult for TiO_2@PEGDA hydrogel to adsorb bisphenolate anions due to repulsive electrostatic interactions.

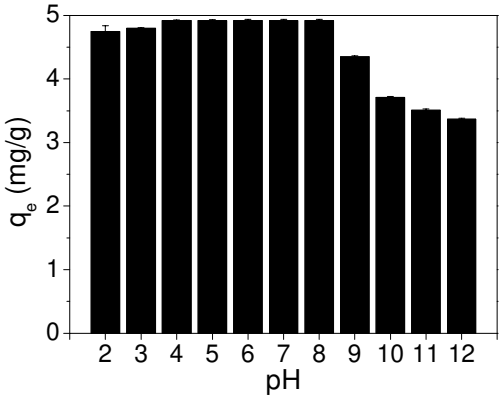

Fig. 7 Effect of pH on BPA adsorption (BPA = 25mg/L)

Effect of time and kinetics study

The changes of BPA adsorption capacity according to reaction time was displayed in Fig. 8a. It was rapid for BPA adsorbed on TiO_2@PEGDA at the first 6 min and became slower later. The capacity remained stable after 12 min, and the equilibrium absorption capacity was 4.92 mg/g. At the initial process, the adsorption active sites were abundant for catching BPA, and they were gradually occupied until reaching balance.

For investigating the kinetic characteristic, pseudo-first-order model and the pseudo-second-order model were used for analyzing adsorption process.

The pseudo-first-order model is written by Eq. (4).

$$ln(q_e - q_t) = lnq_e - K_1 t \quad (4)$$

Where q_t and q_e (mg/g) stand for the adsorption capacity at any given time and equilibrium time, respectively. K_1 is the rate constant (1/min). Both q_e and K_1 can be calculated from the intercept and slope of the plot of $ln\ (q_e - q_t)$ versus t, respectively.

The pseudo-second-order model is presented by Eq. (5).

$$\frac{t}{q_t} = \frac{1}{K_2 q_e^2} + \frac{t}{q_e} \quad (5)$$

Where K_2 (g/(mg·min)) stands for the rate constant of the pseudo-second-order model.

BPA adsorption kinetic parameters were shown in Table 2. According to the correlation coefficients, the pseudo-second order model (R^2 = 0.9990) was more suitable for BPA adsorption process than the pseudo-first model (R^2 = 0.4202), indicating that the adsorption rate is proportional to the square of the number of unoccupied sites on TiO_2@PEGDA, and the functionality plays the major role in adsorption rather than the structural characteristic of the hydrogels. Furthermore, $q_{e,cal}$ (4.90 mg/g) calculated by the pseudo-second order kinetic model was much closer to the experimental capacity ($q_{e,exp}$ = 4.92 mg/g).

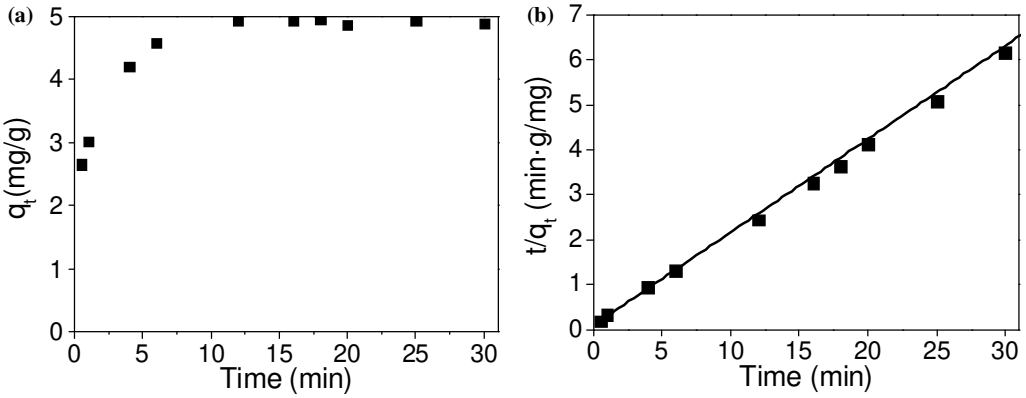

Fig. 8 **a** Effect of time on BPA adsorption (BPA = 25 mg/L). **b** Pseudo-second-order model fitting

Table 2 BPA adsorption kinetic parameters

Kinetic models	$q_{e,cal}$ (mg/g)	K_1 (1/min)	K_2 (g/(mg·min))	R^2
Pseudo-first-order model	1.87	0.12	/	0.4202
Pseudo-second-order model	4.90	/	0.48	0.9990

Effect of initial concentration and adsorption isotherms

Fig. 9 showed the trends of q_e at different given concentration of BPA. The adsorption capacity was improved significantly with increased initial concentration, and the values of q_e were 4.92, 9.45, 20.14, 40.29, 61.78, 101.40, 155.02 and 174.58 mg/g, respectively. It is easy for BPA molecular to overcome mass transfer resistance between solution and hydrogel adsorbent at higher concentration due to its larger driving force. The hydrogels showed high adsorption capacity, indicating that TiO_2@PEGDA is a favorable alternative to adsorb BPA.

The Langmuir and the Freundlich model were adopted for studying adsorption isotherms. Eq. (6) and Eq. (7) explain the linear isotherm model for Langmuir and Freundlich, respectively.

The Langmuir model:

$$\frac{C_e}{q_e} = \frac{1}{q_{max} K_L} + \frac{C_e}{q_{max}} \tag{6}$$

Where q_{max} (mg/g) stands for the maximum equilibrium adsorption capacity and K_L (L/g) corresponds to the adsorption equilibrium constant.

The Freundlich model:

$$\ln q_e = \frac{1}{n} \ln C_e + \ln K_F \tag{7}$$

Where n is the number of active sites of TiO_2@PEGDA required for one BPA to adsorb, and K_F ((mg/g)(L/mg)$^{1/n}$) corresponds to the adsorption equilibrium constant.

The parameters of adsorption isotherms were presented in Table 3. As we can see from correlation coefficient R^2, adsorption process fitted well to the Freundlich model (R^2 = 0.9879), indicating that the interaction between adsorbed BPA and heterogeneous surfaces of TiO_2@PEGDA mainly functioned. And it was favorable for BPA adsorbed on TiO_2@PEGDA as *1/n* was bigger than 1.

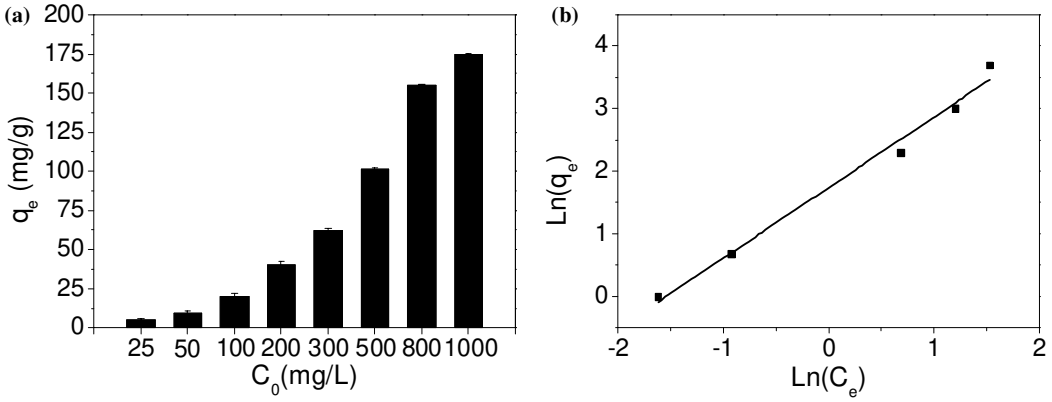

Fig. 9 **a** Effect of initial concentration on BPA adsorption. **b** Freundlich isotherm model

Table 3 The isotherm model parameters

Freundlich isotherm		Langmuir isotherm	
K_F (mg/g)(L/mg)$^{1/n}$	5.68	q_{max} (mg/g)	5.55
1/n	1.13	K_L (L/g)	0.084
R^2	0.9879	R^2	0.8155

Effect of temperature and thermodynamic parameters

In order to study thermodynamic characteristics, adsorption experiments were conducted at 277, 298 and 313 K. Thermodynamic parameters, including Gibbs free energy (ΔG^0, kJ/mol), Enthalpy (ΔH^0, kJ/mol) and Entropy (ΔS^0, kJ/(mol·K)) were calculated as follows.

$$\triangle G_0 = -RTlnK_0 \quad (8)$$

$$lnK_0 = \frac{\triangle S^0}{R} - \frac{\triangle H^0}{RT} \quad (9)$$

$$\triangle H^0 = \triangle G^0 + T\triangle S^0 \quad (10)$$

Where R (8.314 J/(mol·K)) and T (K) correspond to the universal gas constant and the solution temperature, respectively. K_0 (L/mol) can be calculated from the slope of the plot of $ln\ (q_e/C_e)$ versus C_e.

The results were shown in Table 4. The values of ΔG^0 were –2.95, –2.99 and –3.03 at 277 K, 298 K and 318 K, respectively. These negative values indicated that it was a spontaneous process when BPA adsorbed on TiO_2@PEGDA, and rather than the chemical adsorption, the physical adsorption was the primary mechanism. The value of ΔH^0 was negative also, reflecting that it was an exothermic adsorption, thus the adsorption ability weakened with elevated temperature as presented in Fig. 10. The positive ΔS^0 indicated that randomness was increased at the adsorbed BPA-TiO_2@PEGDA surface during the adsorption process.

Table 4 Thermodynamic parameters for BPA adsorbed on TiO_2@PEGDA

T (K)	ΔG^0 (kJ/mol)	ΔH^0 (kJ/mol)	ΔS^0 (kJ/(mol·K))
277	–2.95	–2.46	0.0018
298	–2.99		
318	–3.03		

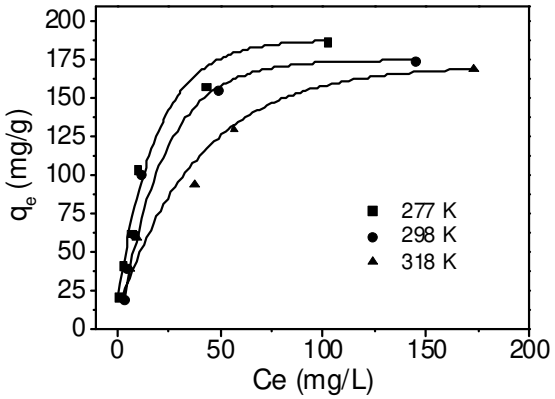

Fig. 10 Effect of temperature on BPA adsorption

Photocatalysis regeneration of TiO_2@PEGDA for repetitive use

As mentioned before, a major advantage of TiO_2 immobilization on the hydrogels as filler is its eco-friendly recovery. After the first adsorption, the BPA-adsorbed hydrogels were collected, and left to UV illumination for in-situ photocatalytic oxidation to desorb BPA from hybrid hydrogels. Afterwards, the same hydrogels were used for next fresh BPA adsorption process. The result was presented in Fig. 11. In the first and the second adsorption cycles, complete removal of BPA occurred. After the third cycle, decrease in adsorption efficiency was evident, but it still stayed at a satisfactory level of 92.5% relative to initial adsorption capacity. Further decrease was seen in the forth cycle (85.6%). Such decline for adsorption efficiency could be attributed to generated by- and end-product of photocatalysis on hydrogels' surface in previous cycles, which blocking active sites and thus resisting the further adsorption.

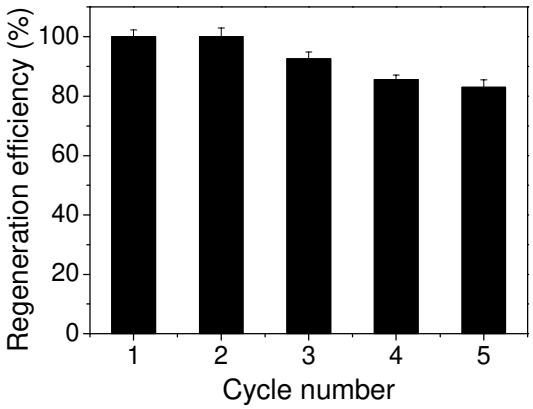

Fig. 11 Reusability of TiO_2@PEGDA

Conclusions

Hybrid hydrogel TiO_2@PEGDA were fabricated by light polymerization. The surface

of spherical hydrogels was rough due to the introduced TiO_2. They exhibited limited crystallinity and various functional groups. Due to the presence of TiO_2, the adsorption capacity was slightly increased, whereas swelling property was decreased. The adsorption capacity decreased obviously at pH $>$ 8.0, and improved significantly by increasing the initial concentration of BPA. The adsorption process was fitted well with the pseudo-second-order kinetic and the Freundlich isotherm model. Thermodynamic data proved that BPA adsorbed on TiO_2@PEGDA was spontaneous and exothermic. BPA was degraded from adsorption-saturated hybrid hydrogels under UV light irradiation, and the regenerated TiO_2@PEGDA can be repeatedly used for several cycles without significant adsorption capacity loss. We wish this work will encourage further studies of hybrid hydrogels with self-regeneration property for efficient and eco-friendly elimination of BPA.

Declarations

Ethics approval and consent to participate

Not applicable.

Consent for publication

Not applicable.

Availability of data and materials

Not applicable.

Competing interests

The authors declare that they have no known competing financial interests or personal relationships that could have appeared to influence the work reported in this paper.

Funding

This work was supported by Education Department of Jilin Province of China (JJKH20200425KJ), and Department of Science and Technology of Jilin Province of China (20190303071SF).

Authors' contributions

Mingyue Piao (writing, editing and funding acquisition), Hongxue Du (investigation and data curation), Yuwei Sun (investigation and methodology), Honghui Teng (supervision and funding acquisition).

References

Almeida TFA, Oliveira SR, Mayra da Silva J, Fernandes de Oliveira AL, de Lourdes Cardeal Z, Menezes HC et al (2021) Effects of high-dose bisphenol A on the mouse oral mucosa: a possible link with oral cancers. Environ Pollut 286:117296. https://doi.org/10.1016/j.envpol.2021.117296

Ashfaq M, Sun Q, Zhang H, Li Y, Wang YW, Li MY et al (2018) Occurrence and fate of bisphenol A transformation products, bisphenol A monomethyl ether and bisphenol A dimethyl ether, in wastewater treatment plants and surface water. J Hazard Mater 357:401-407. https://doi.org/10.1016/j.jhazmat.2018.06.022

Biemann R, Blüher M, Isermann B (2021) Exposure to endocrine-disrupting compounds such as phthalates and bisphenol A is associated with an increased risk for obesity. Best Pract Res Cl En: 101546. https://doi.org/10.1016/j.beem.2021.101546

Chakraborty P, Shappell NW, Mukhopadhyay M, Onanong S, Rex KR, Snow D (2021) Surveillance of plasticizers, bisphenol A, steroids and caffeine in surface

369 water of River Ganga and Sundarban wetland along the Bay of Bengal:
370 occurrence, sources, estrogenicity screening and ecotoxicological risk assessment.
371 Water Res 190:116668. https://doi.org/10.1016/j.watres.2020.116668
372 Chen X, Li PY, Kang Y, Zeng XT, Xie Y, Zhang YK et al (2019) Preparation of
373 temperature-sensitive Xanthan/NIPA hydrogel using citric acid as crosslinking
374 agent for bisphenol A adsorption. Carbohydr Polym 206:94-101.
375 https://doi.org/10.1016/j.carbpol.2018.10.092
376 Dai HJ, Zhang YH, Ma L, Zhang H, Huang HH (2019) Synthesis and response of
377 pineapple peel carboxymethyl cellulose-g-poly (acrylic
378 acid-co-acrylamide)/graphene oxide hydrogels. Carbohydr Polym 215:366-376.
379 https://doi.org/10.1016/j.carbpol.2019.03.090
380 de Souza ÍFT, Petri DFS (2018) β-Cyclodextrin hydroxypropyl methylcellulose
381 hydrogels for bisphenol A adsorption. J Mol Liq 266:640-648.
382 https://doi.org/10.1016/j.molliq.2018.06.117
383 Du HX, Piao MY (2018) Facile preparation of microscale hydrogel particles for high
384 efficiency adsorption of bisphenol A from aqueous solution. Environ Sci Pollut
385 Res 25:28562-28571. https://doi.org/10.1007/s11356-018-2879-0
386 Glass S, Trinklein B, Abel B, Schulze A (2018) TiO_2 as photosensitizer and
387 photoinitiator for synthesis of photoactive TiO_2-PEGDA hydrogel without organic
388 photoinitiator. Front Chem 6:340-349. https://doi.org/10.3389/fchem.2018.00340
389 Hunge YM, Yadav AA, Khan S, Takagi K, Suzuki N, Teshima K et al (2021)
390 Photocatalytic degradation of bisphenol A using titanium dioxide@nanodiamond
391 composites under UV light illumination. J Colloid Interface Sci 582:1058-1066.
392 https://doi.org/10.1016/j.jcis.2020.08.102
393 Kumar A, Zo SM, Kim JH, Kim S-C, Han SS (2019) Enhanced physical, mechanical,

394 and cytocompatibility behavior of polyelectrolyte complex hydrogels by
395 reinforcing halloysite nanotubes and graphene oxide. Compos Sci Technol
396 175:35-45. https://doi.org/10.1016/j.compscitech.2019.03.008
397 Kuo C-Y (2009) Comparison with as-grown and microwave modified carbon
398 nanotubes to removal aqueous bisphenol A. Desalination 249:976-982.
399 https://doi.org/10.1016/j.desal.2009.06.058
400 Lin Q, Wu YY, Jiang X, Lin FC, Liu X, Lu BL (2019) Removal of bisphenol A from
401 aqueous solution via host-guest interactions based on beta-cyclodextrin grafted
402 cellulose bead. Int J Biol Macromol 140:1-9.
403 https://doi.org/10.1016/j.ijbiomac.2019.08.116
404 Liu JC, Zhang LY, Lu GH, Jiang RR, Yan ZH, Li YP (2021) Occurrence, toxicity and
405 ecological risk of bisphenol A analogues in aquatic environment: a review.
406 Ecotoxicol Environ Saf 208:111481. https://doi.org/10.1016/j.ecoenv.2020.111481
407 Liu XX, Chang MM, He B, Meng L, Wang XH, Sun RC et al (2019) A one-pot
408 strategy for preparation of high-strength carboxymethyl xylan-g-poly(acrylic acid)
409 hydrogels with shape memory property. J Colloid Interface Sci 538:507-518.
410 https://doi.org/10.1016/j.jcis.2018.12.023
411 Marrakchi F, Fazeli Zafar F, Wei MM, Wang S (2021) Cross-linked $FeCl_3$-activated
412 seaweed carbon/MCM-41/alginate hydrogel composite for effective biosorption of
413 bisphenol A plasticizer and basic dye from aqueous solution. Bioresour Technol
414 331:125046. https://doi.org/10.1016/j.biortech.2021.125046
415 Moon S, Yu SH, Lee CB, Park YJ, Yoo HJ, Kim DS (2021) Effects of bisphenol A on
416 cardiovascular disease: an epidemiological study using National Health and
417 Nutrition Examination Survey 2003–2016 and meta-analysis. Sci Total Environ
418 763:142941. https://doi.org/10.1016/j.scitotenv.2020.142941

419 Mpatani FM, Han R, Aryee AA, Kani AN, Li Z, Qu L (2021) Adsorption performance
420 of modified agricultural waste materials for removal of emerging
421 micro-contaminant bisphenol A: a comprehensive review. Sci Total Environ
422 780:146629. https://doi.org/10.1016/j.scitotenv.2021.146629
423 Santhi VA, Sakai N, Ahmad ED, Mustafa AM (2012) Occurrence of bisphenol A in
424 surface water, drinking water and plasma from Malaysia with exposure
425 assessment from consumption of drinking water. Sci Total Environ
426 427-428:332-338. https://doi.org/10.1016/j.scitotenv.2012.04.041
427 Sundarraj S, Sujitha MV, Alphonse CRW, Kalaiarasan R, Kannan RR (2021)
428 Bisphenol A alters hematopoiesis through EGFR/ERK signaling to induce
429 myeloblastic condition in zebrafish model. Sci Total Environ 787:147530.
430 https://doi.org/10.1016/j.scitotenv.2021.147530
431 Van den Broeck L, Piluso S, Soultan AH, De Volder M, Patterson J (2019)
432 Cytocompatible carbon nanotube reinforced polyethylene glycol composite
433 hydrogels for tissue engineering. Mater Sci Eng C Mater Biol Appl 98:1133-1144.
434 https://doi.org/10.1016/j.msec.2019.01.020
435 Wang YQ, Aimuzi R, Nian M, Zhang Y, Luo K, Zhang J (2021) Bisphenol A
436 substitutes and sex hormones in children and adolescents. Chemosphere
437 278:130396. https://doi.org/10.1016/j.chemosphere.2021.130396
438 Xu YW, Hu AL, Li YR, He Y, Xu JM, Lu ZJ (2021) Determination and occurrence of
439 bisphenol A and thirteen structural analogs in soil. Chemosphere 277:130232.
440 https://doi.org/10.1016/j.chemosphere.2021.130232
441 Zhou AJ, Chen WW, Liao L, Xie PC, Zhang TC, Wu XM et al (2019) Comparative
442 adsorption of emerging contaminants in water by functional designed magnetic
443 poly(N-isopropylacrylamide)/chitosan hydrogels. Sci Total Environ 671:377-387.

444 https://doi.org/10.1016/j.scitotenv.2019.03.183
445 Zhu HJ, Li ZK, Yang JH (2018) A novel composite hydrogel for adsorption and
446 photocatalytic degradation of bisphenol A by visible light irradiation. Chem Eng J
447 334:1679-1690. https://doi.org/10.1016/j.cej.2017.11.148